390968-1-T

Scattering by a planar resistive strip array

John L. Volakis and Y.-C. Lin

Northrop Corporation
B2 Division
8900 E. Washington Blvd.
Pico Rivera CA

September 1992
Revised October 1992

390968-1-T = RL-2579

Scattering by a planar resistive strip array

J. L. Volakis and Y.-C. Lin

Radiation Laboratory
Department of Electrical Engineering
and Computer Science
The University of Michigan
Ann Arbor MI 48109-2122

July 17, 1992
First Revision August 3, 1992
Second Revision October 27, 1992

Abstract

In this report we consider the scattering by an infinite resistive strip grating subjected to an H-polarized plane wave incidence. An approximate analytic solution is obtained on the assumption of a small width strip array and this solution is verified by comparison with moment method data. Following the proposed solution, equivalent complex impedance and power loss formulae are derived and numerical results are included.

Problem description

Consider the infinite array of resistive strips illustrated in Figure 1. The strips occupy the xz plane, have a resistivity R, are of width w, and the array period is T. On the assumption that $w \ll \lambda$, we are interested in the reflectivity of the strip array when illuminated by an H-polarized plane wave. That is, the incident field is of the form

$$\begin{aligned} \mathbf{E}^i &= (\hat{x}\sin\phi_0 - \hat{y}\cos\phi_0) Z_0 e^{jk(x\cos\phi_0 + y\sin\phi_0)} \\ \mathbf{H}^i &= \hat{z} e^{jk(x\cos\phi_0 + y\sin\phi_0)} \end{aligned} \tag{1}$$

where $k = 2\pi/\lambda$ is the free space wavenumber and Z_0 is the free space intrinsic impedance.

Analysis procedure

A standard procedure for determining the reflected/scattered field by the strip arrays is to first find the current on the periodic array of strips. Because the array is periodic, Floquet's theorem requires that the current distribution be also periodic for uniform amplitude illumination (except for a phase factor). As a result, the computational domain can be confined to a single period, thus, substantially simplifying the analysis. With this understanding, an appropriate integral equation can be constructed by imposing the resistive transition condition and the aforementioned periodicity requirements. For small strip widths, it is possible to arrive at a closed form solution for the strip currents using the procedure described by Barkeshli and Volakis [1]. Once the current is found, the scattered field is readily evaluated. In accordance with Floquet's theorem, this will be comprised of a sum of discrete plane wave harmonics (Floquet harmonics), and thus of interest is the evaluation of the amplitudes, phase and propagation characteristics of these harmonics. When the period $T < \lambda/2$, which is the case of most interest here, only a single reflected and transmitted harmonic is possible.

Integral equation

Based on Floquet's theorem, the current on the periodic array of resistive strips satisfies the periodicity requirement

$$J_x(x + nT) = J_x(x)\, e^{+jknT\cos\phi_0}; \qquad n = 0, \pm 1, \pm 2, \pm 3, \ldots \tag{2}$$

where $J_x(x)$ is the current on the strip centered at the origin, and the phase factor accounts for the delay or advance of the incident plane wave at the nth strip. Thus, the total current on the strip array is given by the sum

$$\sum_{n=-\infty}^{\infty} J_x(x)\, e^{+jknT\cos\phi_0}$$

which implies the scattered field representation

$$\begin{aligned} E_x^s(x,y) &= -\frac{kZ}{4}\sum_{n=-\infty}^{\infty}\int_{-w/2}^{w/2} J_x(x')\, e^{+jknT\cos\phi_0} \\ &\quad \cdot\left(1+\frac{1}{k^2}\frac{\partial^2}{\partial x^2}\right) H_0^{(2)}\left(k\sqrt{(x-x'-nT)^2+y^2}\right)\, dx' \end{aligned}$$

It is convenient to introduce the periodic Green's function

$$G(x,x',y) = -\frac{j}{4}\sum_{n=-\infty}^{\infty} H_0^{(2)}\left(k\sqrt{(x-x'-nT)^2+y^2}\right)\, e^{+jknT\cos\phi_0}. \qquad (3)$$

We can then rewrite the scattered field in a more compact form as

$$E_x^s(x,y) = -jkZ\int_{-w/2}^{w/2} J_x(x')\left(1+\frac{1}{k^2}\frac{\partial^2}{\partial x^2}\right) G(x,x',y)\, dx' \qquad (4)$$

The sum (3) is very slowly converging but can be recast in a more computationally attractive form by noting that

$$H_0^{(2)}\left(k\sqrt{x^2+y^2}\right) = \frac{1}{\pi}\int_{-\infty}^{\infty} \frac{e^{-j\sqrt{k^2-\alpha^2}|y|}}{\sqrt{k^2-\alpha^2}}\, e^{j\alpha x}\, d\alpha \qquad (5)$$

with the branch of the root such that $\mathrm{Im}\left(\sqrt{k^2-\alpha^2}\right) < 0$. This expression can be substituted into (3), and upon interchanging the order of integration and summation we have

$$G(x,x',y) = \frac{-j}{4\pi}\int_{-\infty}^{\infty} \frac{e^{-j\left\{\sqrt{k^2-\alpha^2}|y|+\alpha(x-x')\right\}}}{\sqrt{k^2-\alpha^2}}\left\{\sum_{n=-\infty}^{\infty} e^{jn(\alpha+k\cos\phi_0)T}\right\} d\alpha \qquad (6)$$

Next, on invoking the identity

$$\sum_{n=-\infty}^{\infty} e^{+jn(\alpha+k\cos\phi_0)T} = 2\pi\sum_{n=-\infty}^{\infty}\delta[(\alpha+k\cos\phi_0)T+2\pi n] \qquad (7)$$

where $\delta(x)$ is the usual Dirac function, we can express $G(x, x', z)$ by the sum

$$G(x, x', y) = \frac{-j}{2T} \sum_{n=-\infty}^{\infty} \frac{e^{-j\sqrt{k^2-\beta_n^2}|y|}}{\sqrt{k^2-\beta_n^2}} e^{+j\beta_n(x-x')} \tag{8}$$

where $\beta_n = \frac{2\pi n}{T} + k\cos\phi_0$. Clearly, this expression converges faster than that in (3).

Having a suitable expression for the scattered field, an integral equation for the current on a single periodic strip is now readily constructed by imposing the transition condition

$$E_x^i(x, y=0) + E_x^s(x, y=0) = RJ_x(x) \tag{9}$$

for $-w/2 < x < w/2$. On using (4) along with (8) into (9) we obtain

$$\sin\phi_0 e^{jkx\cos\phi_0} = \frac{RJ_x(x)}{Z_0} + \frac{1}{2kT} \sum_{n=-\infty}^{\infty} I_n \sqrt{k^2-\beta_n^2}\, e^{j\beta_n x} \tag{10}$$

where

$$I_n = \int_{-w/2}^{w/2} J_x(x')\, e^{-j\beta_n x'}\, dx'. \tag{11}$$

Equation (10) is an integral equation to be enforced over $-w/2 < x < w/2$ for a determination of the current $J_x(x)$. Below we consider two different solutions of (10). One is based on a standard method of moments using pulse basis and point matching whereas the other is an approximate analytic solution which becomes more accurate as the width of the strip decreases. The numerical solution of (10) has been considered by Sarabandi [1] and will only be used here to evaluate the accuracy of the proposed analytic approximation.

Approximate solution

Recently, Barkeshli and Volakis [2] considered the scattering by a narrow groove in a ground plane, a problem closely related to that of scattering by a single impedance and/or resistive insert and strip. Based on this study, we conjecture that the current on a narrow strip can be represented by the expression

$$J_x(x) = A\sqrt{1-\left(\frac{2x}{w}\right)^2}\, e^{jkx\cos\phi_0} \tag{12}$$

where A is a constant to be determined. Substituting this into (11) we get

$$\begin{aligned} I_n &= A\int_{-w/2}^{w/2}\sqrt{1-\left(\frac{2x}{w}\right)^2}\,e^{j(k\cos\phi_0-\beta_n)x'}\,dx' \\ &= A\frac{T}{2n}J_1\left(n\frac{w\pi}{T}\right) \end{aligned} \tag{13}$$

in which J_1 denotes the first order Bessel function. Next, following Galerkin's procedure we multiply both sides of (10) by $\sqrt{1-\left(\frac{2x}{w}\right)^2}\,e^{-jkx\cos\phi_0}$ and upon integrating over the computational domain we have

$$\begin{aligned} \sin\phi_0\int_{-w/2}^{w/2}\sqrt{1-\left(\frac{2x}{w}\right)^2}\,dx &= A\frac{R}{Z_0}\int_{-w/2}^{w/2}\left[1-\left(\frac{2x}{w}\right)^2\right]dx \\ &\quad+\frac{1}{2kT}\sum_{n=-\infty}^{\infty}I_n\sqrt{k^2-\beta_n^2} \\ &\quad\cdot\int_{-w/2}^{w/2}\sqrt{1-\left(\frac{2x}{w}\right)^2}\,e^{-jkx\cos\phi_0}e^{j\beta_n x}\,dx. \end{aligned}$$

Carrying out the first two integrals and noting that the third is equal to I_n/A, it follows that

$$A=\sin\phi_0\frac{\pi w/4}{\frac{R}{Z_0}\frac{2w}{3}+\frac{T}{8k}\sum_{n=-\infty}^{\infty}\frac{\sqrt{k^2-\beta_n^2}}{n^2}J_1^2\left(n\frac{w\pi}{T}\right)} \tag{14}$$

The sum in this expression is rapidly convergent, and A is thus easily computed in spite of the infinite sum. Note also that the result (14) bypasses the computation of the periodic Green's function which is often troublesome.

The H_z scattered can be found from the radiation integral, i.e.

$$\begin{aligned} H_z^s(x,y) &= -\int_{-w/2}^{w/2}J_x(x')\frac{\partial}{\partial y}G(x,x',y)\,dx' \\ &= \pm\frac{A}{2T}\sum_{n=-\infty}^{\infty}e^{j\sqrt{k^2-\beta_n^2}|y|}e^{j\beta_n x} \\ &\quad\cdot\int_{-w/2}^{w/2}\sqrt{1-\left(\frac{2x'}{w}\right)^2}\,e^{j(k\cos\phi_0-\beta_n)x'}\,dx'. \end{aligned} \tag{15}$$

From the identity (13) we then find that

$$H_z^s(x,y)=\pm A\sum_{n=-\infty}^{\infty}\frac{J_1\left(n\frac{w\pi}{T}\right)}{4n}e^{-j\sqrt{k^2-\beta_n^2}|y|}e^{j\beta_n x},\qquad y\gtrless 0 \tag{16}$$

which is clearly an infinite sum of Floquet plane wave modes. However, in the far zone only a few of these modes will be observed. The particular ones are those modes for which $\beta_n < k$, and for this inequality to hold, it is necessary that

$$-\frac{T}{\lambda}(1+\cos\phi_0) < n < \frac{T}{\lambda}(1-\cos\phi_0) \tag{17}$$

The corresponding propagation angle for each of the modes is

$$\phi_n^s = \begin{cases} \cos^{-1}\left(-\cos\phi_0 - \dfrac{n\lambda}{T}\right) & y > 0 \\ \\ 2\pi - \cos^{-1}\left(-\cos\phi_0 - \dfrac{n\lambda}{T}\right) & y < 0 \end{cases} \tag{18}$$

However, from (17) it is seen that if $T < \lambda/2$ then only the zeroth mode is present in the far zone. The propagation angle is $\phi_0^s = \pi - \phi_0$ for the $y > 0$ region and $\phi_0^s = \pi + \phi_0$ for the $y < 0$ region. As expected, these are the only reflected and transmitted fields. The associated reflection and transmission coefficient for each of the modes is given by

$$R_{Hn} = \frac{I_n}{2T} \tag{19}$$

and

$$T_{Hn} = \begin{cases} -\dfrac{I_n}{2T} & n \neq 0 \\ \\ 1 - \dfrac{I_0}{2T} & n = 0 \end{cases} \tag{20}$$

with I_n as given by (13). For $T < \lambda/2$, we can replace the periodic array of strips by an equivalent planar resistive sheet which is associated with the same reflection or transmission coefficient given above for the zeroth mode. To do this we recall that the reflection coefficient for a resistive sheet is

$$\Gamma = \frac{\sin\phi_0}{\sin\phi_0 + \dfrac{2R_{\text{eq}}}{Z_0}} \tag{21}$$

where R_{eq} denotes the resistivity of the equivalent sheet. Upon equating this to (19) we find that

$$\frac{R_{\text{eq}}}{Z_0} = \frac{1}{2}\sin\phi_0\left(\frac{1}{R_{H0}} - 1\right) \tag{22}$$

This is the quantity plotted later in the results section, and it will be seen that R_{eq} is essentially independent of the incidence angle ϕ_0.

Another quantity of interest is the power dissipated in the resistive strips. Noting that R in (9) has unites of Ohms/square, we have that the average power dissipated in a length l of an incremental strip of width dx is

$$dP = \frac{1}{2}|I|^2 \frac{R}{l}\, dx = \frac{1}{2}|J_x|^2 l R\, dx \tag{23}$$

From this and (12), we find that the average power dissipated per unit length of a single periodic strip is given by

$$\frac{P}{l} = \frac{1}{2} R \int_{-w/2}^{w/2} \left(1 - \left(\frac{2x}{2}\right)^2\right) dx = |A|^2 \frac{Rw}{3} \tag{24}$$

In the next section we present some numerical computations of R_{H0}, T_{H0}, Z_{eq}/Z_0 and P/l defined respectively, in (19), (20), (23) and (24).

Solution Validation/Numerical Results

The analytic solution presented above for the scattering by a periodic strip array is based on an approximate representation of the current distribution. This approximation improves as the strip width becomes smaller, but its accuracy limitations as the strip width increases still needs to be established. To do so, we shall compare the reflection/transmission coefficients based on our small width approximation presented above to the corresponding quantities obtained from a moment method solution described in the Appendix. For these computations we shall plot R_{H0} and T_{H0} as a function of the ratio w/T for different values of the period T, incidence angle ϕ_0 and the resistivity of the strips R. We begin by looking at Figure 3a where we plotted R_{H0} and T_{H0} for $T = 0.2\lambda$ and $\phi_0 = 60°$ with R set equal to zero or 100Ω/square. As seen, the agreement between the moment method data and our small width approximation is excellent for the curves associated with both values of the resistivity. From the comparison in Figure 3b it is also observed that the small width approximation remains valid even when $w/T = 1$ for $T = 0.5\lambda$. That is, the presented approximate solution is reasonably accurate for strip widths up to $\lambda/2$. This conclusion is better drawn from the current density comparisons given in Figure 4. It is seen from the curves in Figure 4 that the current density amplitude as computed by (14) is within 5–10% of the exact (moment method) values for $w < \lambda/4$.

Moreover, (14) improves as the strip resistivity increases or the width decreases. This is important because in contrast, traditional moment method solutions often run into numerical difficulties as the strip width decreases. From the results presented thus far, it is therefore assured that the small width approximation is suitable for calculations where the array period is less than $\lambda/2$ regardless of the strip width w and the value of R. Plots of the reflection coefficient R_{H0} and the transmission coefficient T_{H0} for small values of T (i.e., $T = 0.4\lambda$, 0.3λ, 0.1λ and 0.05λ) are presented in Figures 5 and 6 as a function of w/T. The curves in these figures were computed using the closed form small width approximation and their accuracy is assured on the basis of the validation done earlier. A general observation from these curves is that the reflection and transmission coefficients are both decreasing as the resistivity of the strips increases. It is also apparent that different choices for w and T can lead to better/optimum performance depending on the design criteria.

Given the reflection and transmission coefficients and having validated these, we can now proceed with the computation of impedance and power loss parameters given in (23) and (24) respectively. The equivalent complex resistivity R_{eq} is, of course, directly dependent on R_{H0} whereas P/l is proportional to current density amplitude A. But, since $R_{H0} = A\left(\frac{w\pi}{8T}\right)$, it also follows that the power loss is proportional to the reflection coefficient as well. Not surprisingly, R_{eq} is nearly nearly independent of ϕ_0 and this is illustrated in Figure 7. Plots of R_{eq} as a function of w/T are given in Figure 8 and it was found that the real part of R_{eq} is independent of the period T but a strong function of w/T and the strip resistivity. This is attributed to that the reflected power is only a function of w/T and R, but not on the specific value of T. Also, from Figure 8b we observe that the imaginary party of R_{eq} is capacitive and independent of the strip resistivity which is assumed real. This is again not surprising since for real strip resistivities any capacitance can only be a function of the strip size and separation.

Curves of P/l are presented in Figures 9 to 13. As before, these curves are plotted as a function of w/T (strip width normalized to the period), and each figure corresponds to a single value of the period T. For example, $T = 0.5\lambda$ for Figure 9; $T = 0.3\lambda$ for Figure 10; and so on. Each plot contains four curves corresponding to four different values of the resistivity R, namely $R = 0, 100, 200$ and 300 ohms/square. The power loss for $R = 0$ is, of course, the horizontal axis (i.e., it is zero). Generally, the power loss increases with the resistivity for all values of w/T. However, this statement does not always hold for all values of w/T as can be observed in Figures 9–11. It is clear,

for example, that the trend is reversed when $w/T > 0.8$ for $T = 0.2\lambda$ in the case of the equivalent impedance. This kind of trend reversal can actually be traced to the formula given by (22). It would appear that the reversal occurs when the phase of the reflection coefficient changes sign in which case the growth of the term $\left(\frac{1}{R_{H0}} - 1\right)$ changes direction.

Approximate Solution for $w/T \approx 1$

The employed physical basis expansion given by (12) forces the current distribution to vanish at the edges of the resistive strip which is the natural edge condition. However, as the separation distance between the resistive strip vanishes (i.e. as $\frac{w}{T}$ approaches unity), the appropriate edge condition is to maintain current continuity between the adjacent strips. Clearly, the chosen expansion (12) cannot satisfy this condition making it inappropriate when $\frac{w}{T} \approx 1$. As a result, we found that when $\frac{w}{T}$ approaches unity, the calculated equivalent reactance via (22) is inaccurate and this is demonstrated in Figure 14. Neither our aproximate formula (22) or the expression given by Marcuvitz [3] are of acceptable accuracy as $\frac{w}{T}$ approaches unity, and as seen from Figure 14, the accuracy of these approximations deteriorates with decreasing period T. However, as demonstrated in Figure 15, the resistive part of (22) continues to remain accurate when $\frac{w}{T} \approx 1$. This is important to consider in developing a model for a more accurate evaluation of the equivalent reactance/capacitance of the strip array. As noted earlier, the reactance of the resistive strip array is independent of the resistivity R, whereas the resistive part of R_{eq} is independent of the period. Consequently, in improving the accuracy of the equivalent reactance, we need only consider the perfectly conducting strip array. Babinet's principle or the surface equivalence principle can then be invoked to instead model the strip array as an array of slits of width $a = T - w$. Below we consider the scattering by such an array in an effort to develop an improved formula for the equivalent reactance of the array.

Referring to Figure 1, and in accordance with the equivalence principle, the scattering by the array of slots in a ground plane can be formulated by introducing magnetic currents over the extent of the slit. The field generated by this (periodic) array of currents is given by

$$H_z^s = -jk_0Y_0\frac{|y|}{y}\int_{-a/2}^{a/2} 2M_z(x')\,G(x,x')\,dx' \tag{25}$$

with $G(x,x')$ as defined in (8). On enforcing tangential magnetic field continuity and employing (25), we obtain the integral equation

$$e^{jk_0x\cos\phi_0} = 2jk_0Y_0\int_{-a/2}^{a/2} M_z(x')\,G(x,x')\,dx' \tag{26}$$

To solve (26) for $M_z(x')$ while keeping in mind that $a \to 0$, we introduce the representation

$$M_z(x') = Ae^{jk_0x\cos\phi_0} \tag{27}$$

which is a one-term pulse basis expansion. Upon substitution of (27) and (8) into (26) we have

$$e^{jk_0x\cos\phi_0} = A\sum_{n=-\infty}^{\infty}\frac{k_0Y_0}{T}a\frac{\operatorname{sinc}\left(\frac{n\pi}{T}a\right)}{\sqrt{k_0^2-\beta_n^2}}\,e^{j\beta_nx} \tag{28}$$

Subsequently, on employing Galerkin's testing we obtain

$$A = \frac{1}{\frac{ak_0Y_0}{T}\sum_{n=-\infty}^{\infty}\frac{\operatorname{sinc}^2\left(\frac{n\pi}{T}a\right)}{\sqrt{k_0^2-\beta_n^2}}} \tag{29}$$

The corresponding scattered field can now be evaluated from (25). We have

$$H_z^s = -\frac{k_0Y_0}{T}aA\sum_{n=-\infty}^{\infty}\operatorname{sinc}\left(\frac{n\pi}{T}a\right)\frac{e^{-j\sqrt{k_0^2-\beta_n^2}}e^{j\beta_nx}}{\sqrt{k_0^2-\beta_n^2}} \tag{30}$$

from which we can identify that the reflection coefficient of the zeroth order node ($n=0$) is given by

$$R_{H0} = 1 - Y_0\frac{Aa}{T\sin\phi_0} \tag{31}$$

where the first term of this expression is due to the reflected field from the undisturbed ground plane. From (22), we now find that

$$\frac{R_{\text{eq}}}{Z_0} = \frac{1}{2}\sin\phi_0\left(\frac{1}{R_{H0}}-1\right) \tag{32}$$

and it can be shown that

$$\frac{R_{\text{eq}}}{Z_0} = -j\left\{2k_0\sum_{\substack{n=-\infty\\ n\neq0}}^{\infty}\frac{\operatorname{sinc}^2\left(n\frac{\pi a}{T}\right)}{\sqrt{\beta_n^2-k_0^2}}\right\}^{-1}$$

Clearly, this result demonstrates that the impedance of a metallic strip array is capacitive, as expected. Also for $a=0$, the sum goes to infinity, implying that $R_{\text{eq}}=0$ for this case. Again this is an expected result.

Conclusion

A closed form solution of the scattering by a resistive strip array was presented. The solution is based on the assumption that the width of the strips are small and in particular it was found that the given formulae for the reflection and transmission coefficients are valid for $w < 0.25\lambda$. This conclusion was reached by comparing the results of the small width approximation with moment method data.

Using the derived reflection and transmission coefficients we also presented equivalent impedance sheets for replacing the strip array and a formula was given for the power loss in terms of the reflection coefficients. Several plots were also presented which showed the dependence of the equivalent impedance and power loss on the various parameters characterizing the strip array. It was found that the strip array can be replaced by an equivalent uniform impedance sheet (independent of incidence angle). The real part of the impedance associated with this sheet is independent of the period and its imaginary part is only dependent on the physical layout of the strips (i.e. independent of the strip resistivity). It was shown that the real part of the derived equivalent impedance remained accurate as the separation distance between the strips approached zero. However, the accuracy of the reactive part of the impedance deteriorated as the strips' separation distance decreased and for that case a different (more accurate) formula was derived.

References

[1] K. Sarabandi, "Scattering from variable resistive and impedance sheets," *J. Electromagn. Waves Appl.*, vol. 4, pp. 865–891, 1990.

[2] K. Barkeshli and J.L. Volakis, "Scattering from a narrow rectangular filled groove," *IEEE Trans. Antennas Propagat.*, pp. 804–810, June 1991.

[3] M. Marcuvitz, *Waveguide Handbook,* Peter Peregrinus Ltd.: London, 1986 (p. 280).

List of Figures

Figure 13. Plots of the absorbed power per square wavelength as a function of w/T with $T = 0.05\lambda$.

Figure 14. Reactive part of R_{eq} as a function of w/T. Note that $\text{Im}\{R_{\text{eq}}\}$ is independent of the resistivity R.

Figure 15. Real part of R_{eq} as a function of w/T for different values of R. Note that $\text{Re}\{R_{\text{eq}}\}$ is independent of the period T.

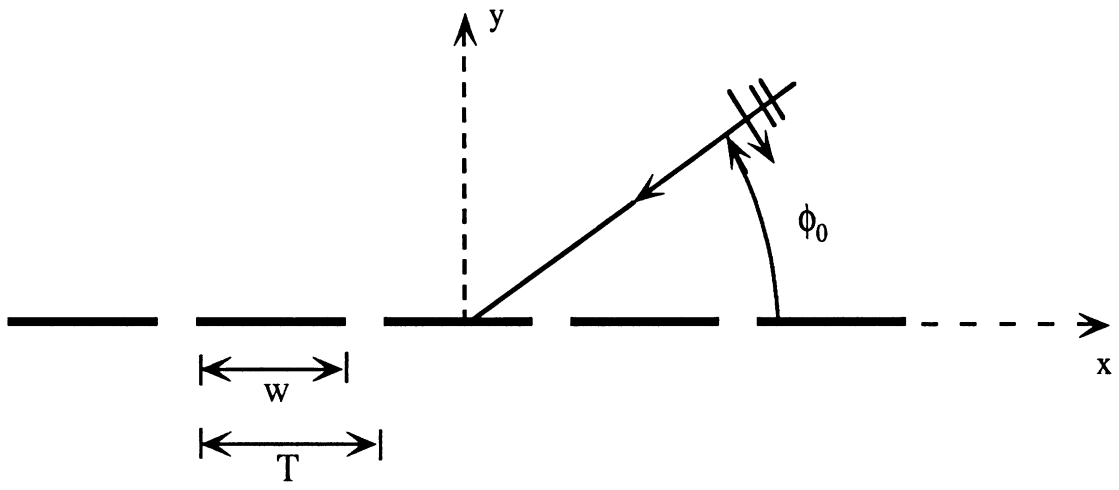

Figure 1. Geometry of the resistive strip array.

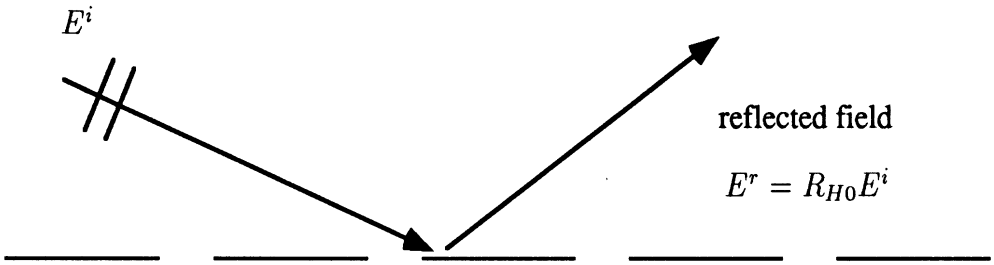

(a) original array of strips

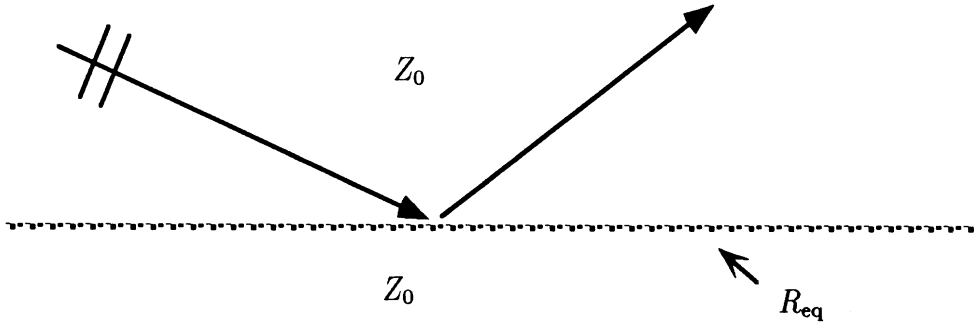

(b) equivalent planar sheet model

Figure 2. Replacement of the strip array by an equivalent resistive sheet.

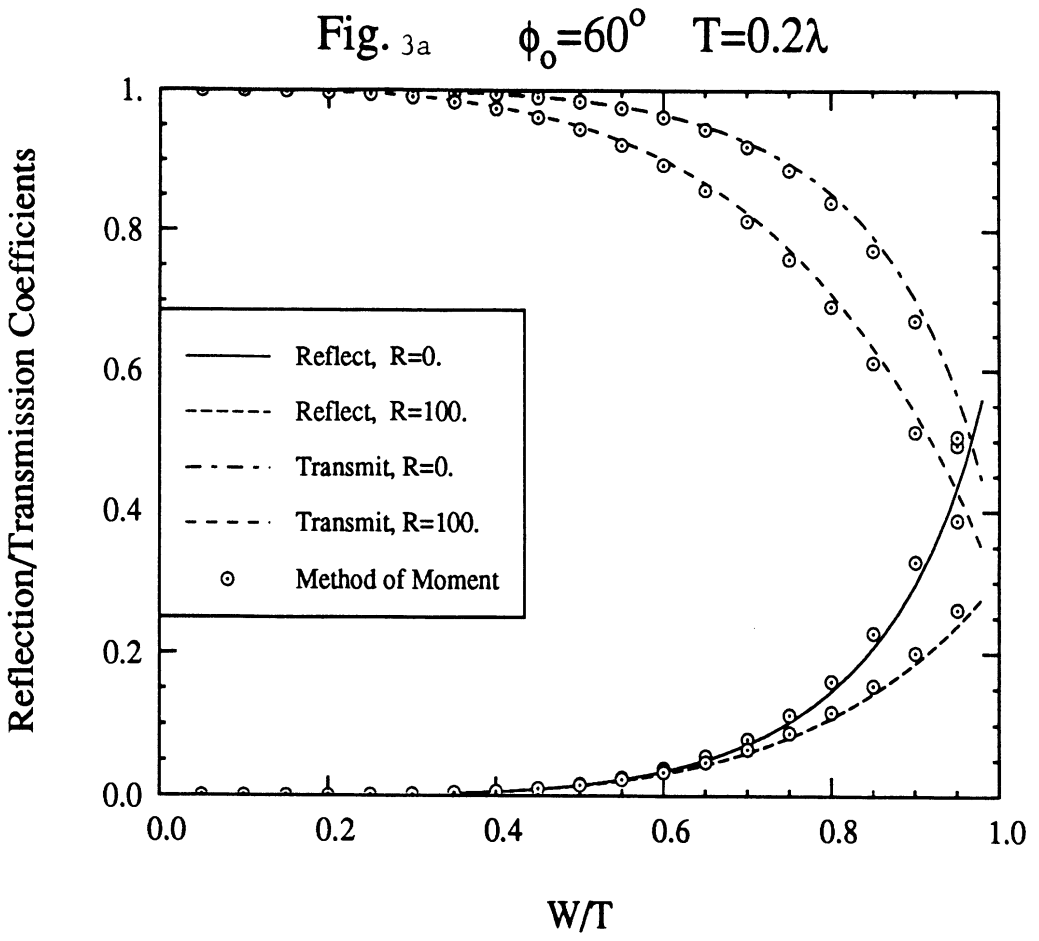

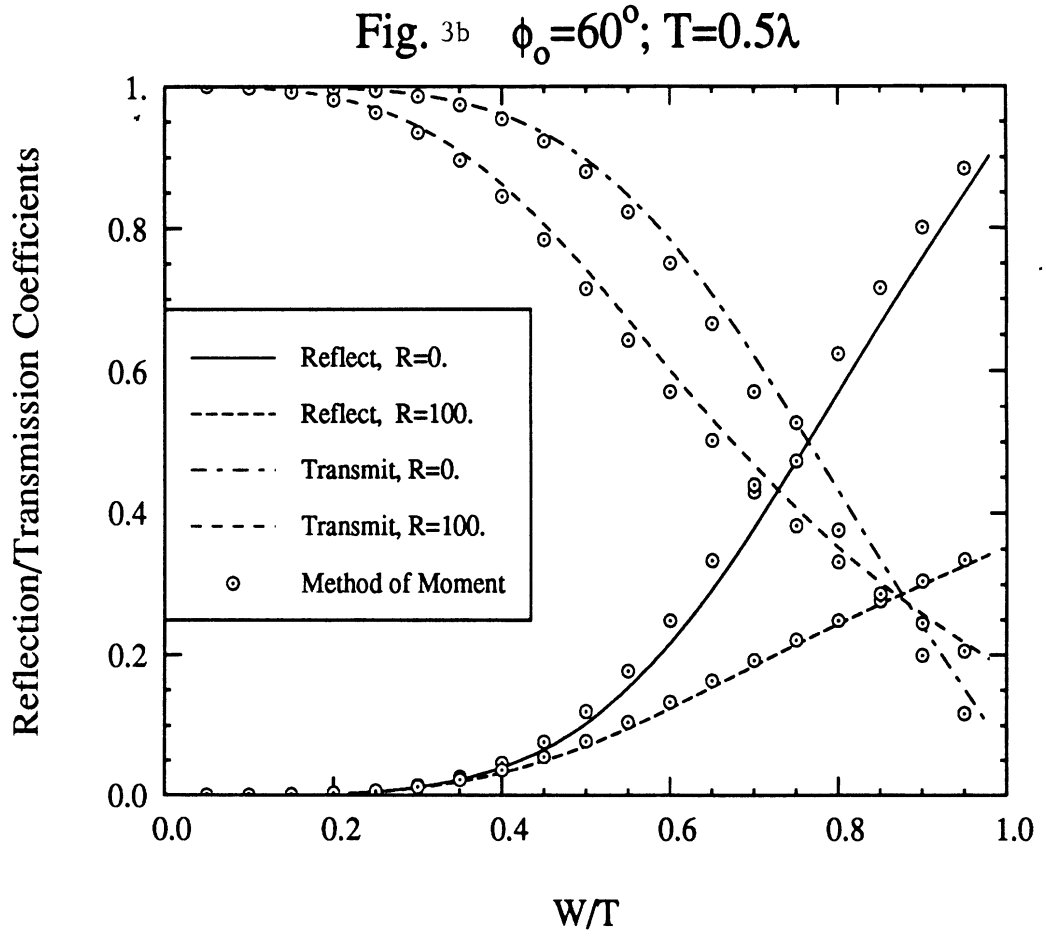

Figure 3. Plots of reflection and transmission coefficients for an infinite resistive strip array as a function of w/T; comparison of the derived closed form formulae (19) and (20) with corresponding moment method data: (a) $T = 0.2\lambda$; (b) $T = 0.5\lambda$.

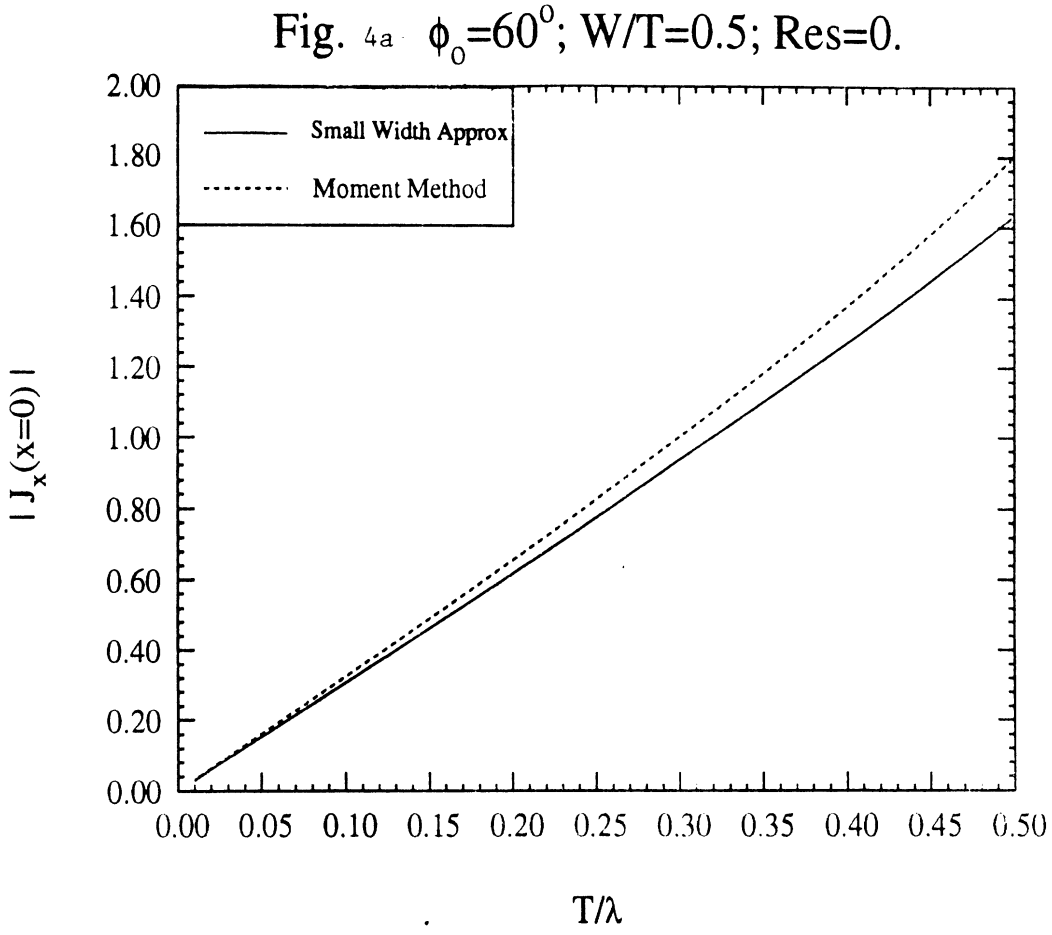

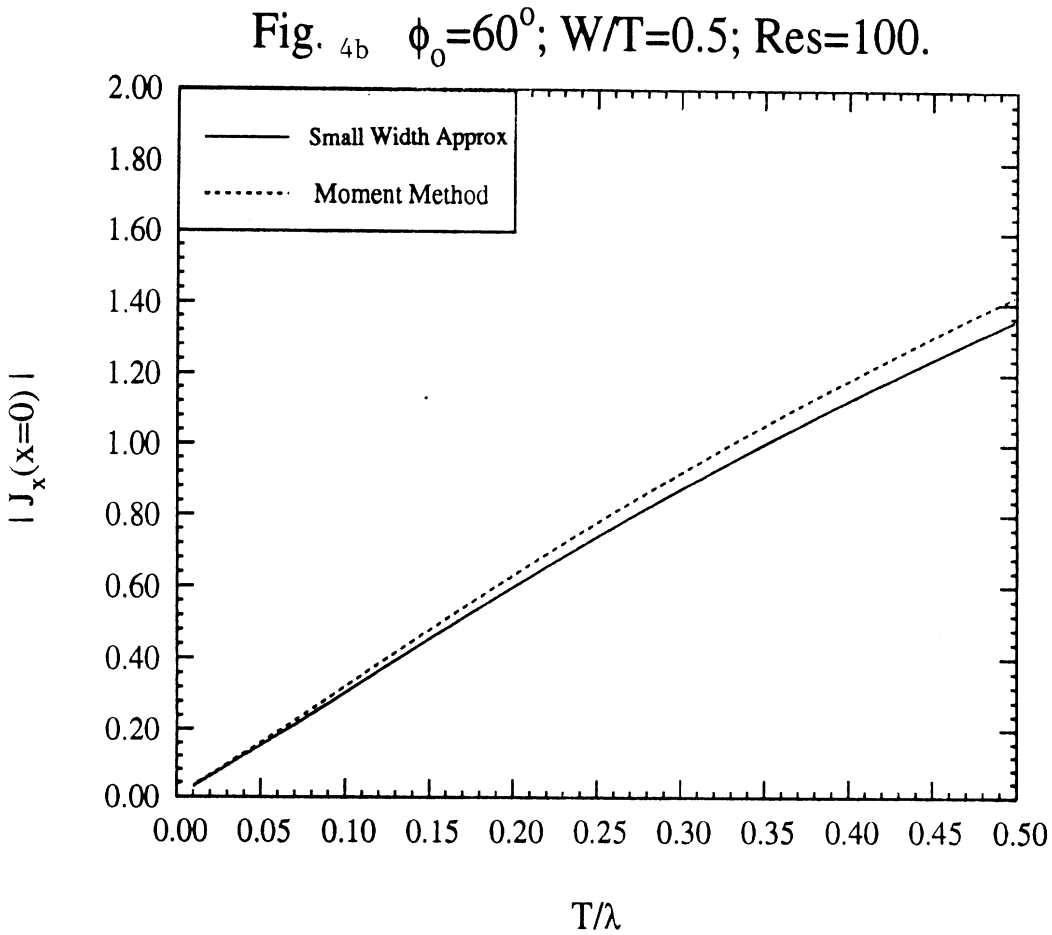

Figure 4. Comparison of the current on the resistive strip array elements as computed by the developed small-width approximation and the moment method.

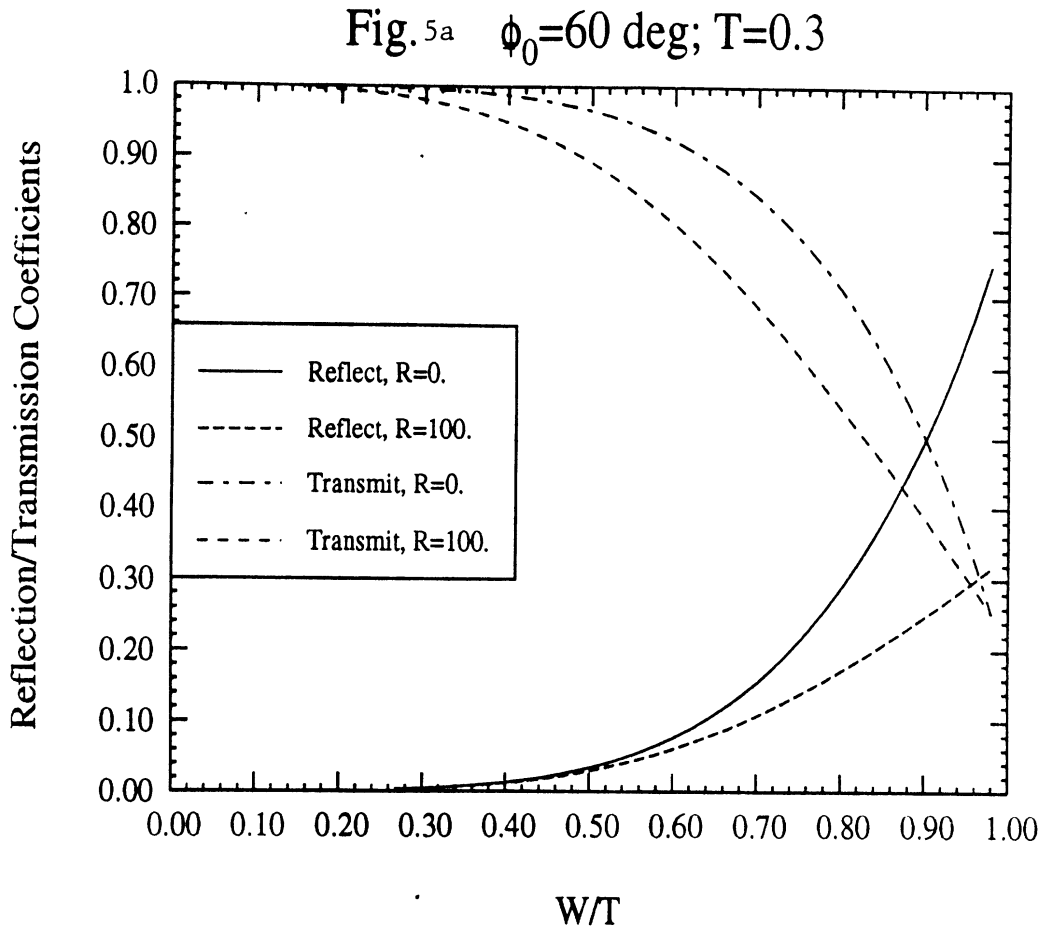

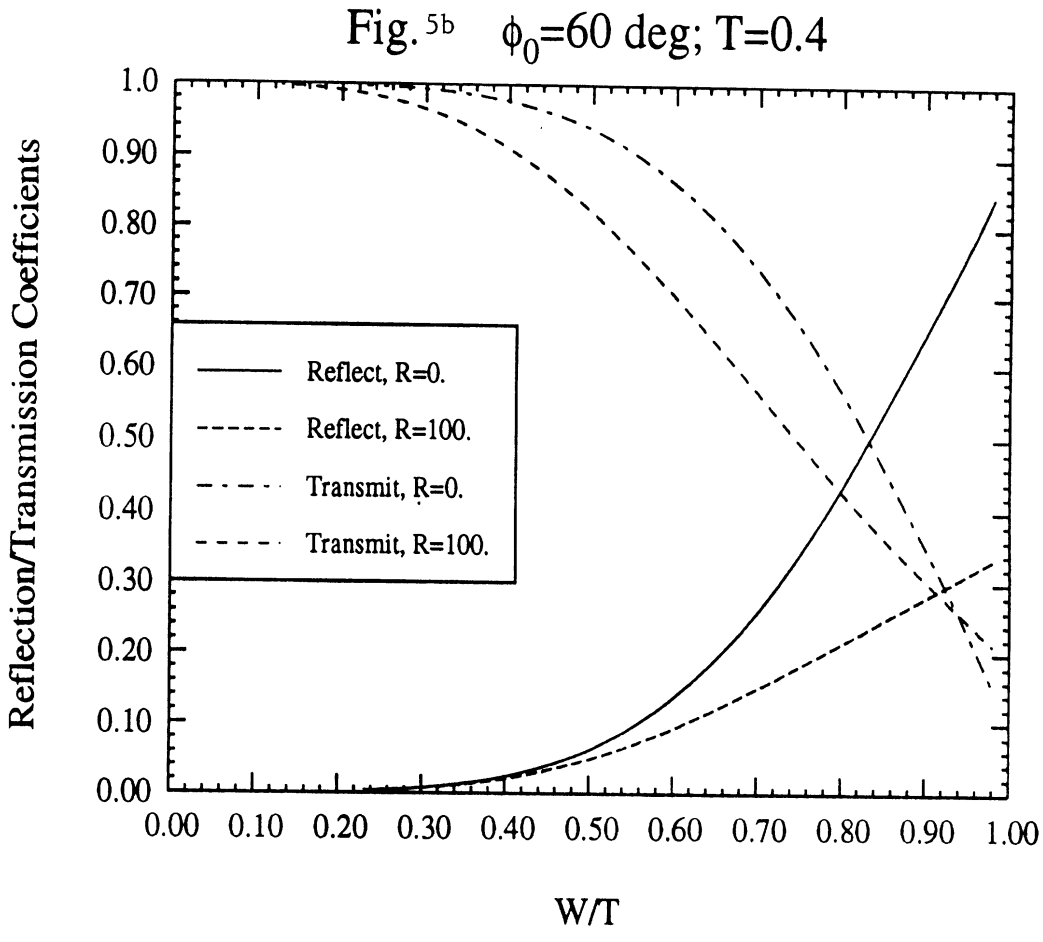

Figure 5. Plots of the reflection and transmission coefficients for an infinite resistive strip array as a function of w/T using the formulae (19) and (20): (a) $T = 0.3\lambda$; (b) $T = 0.4\lambda$.

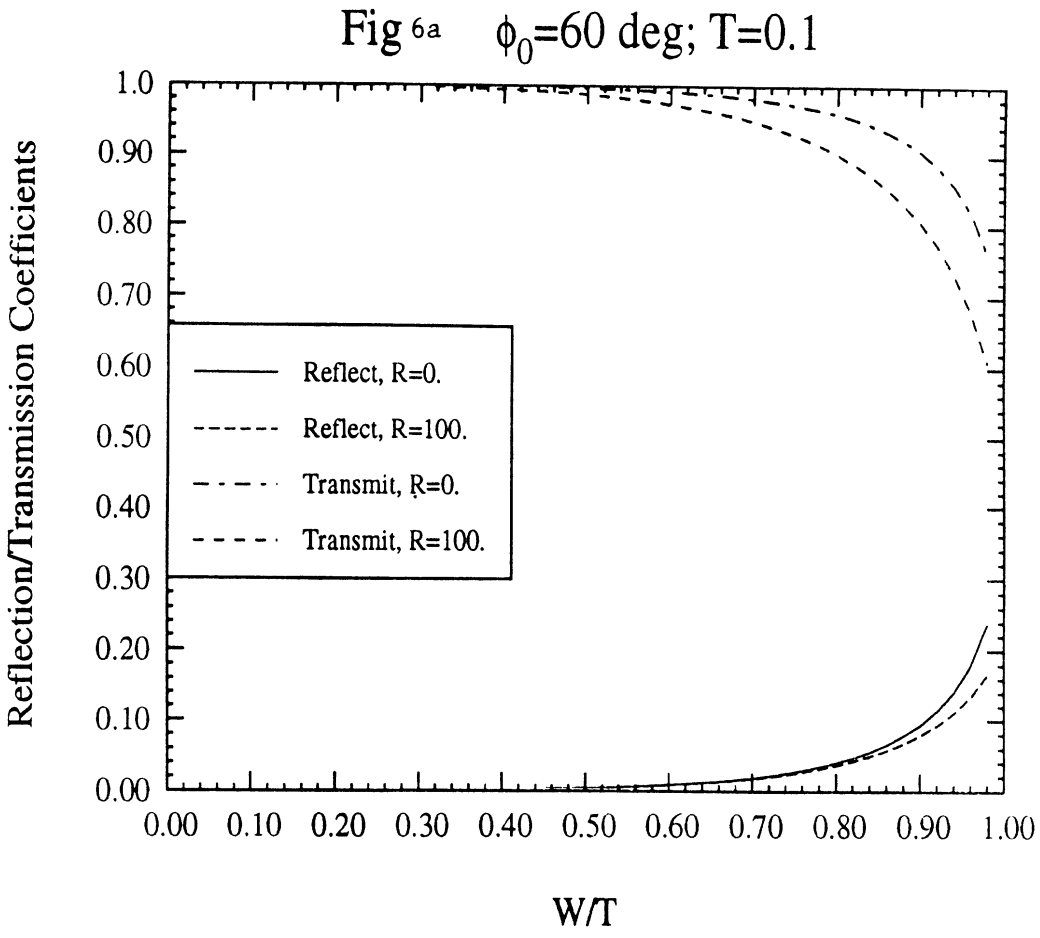

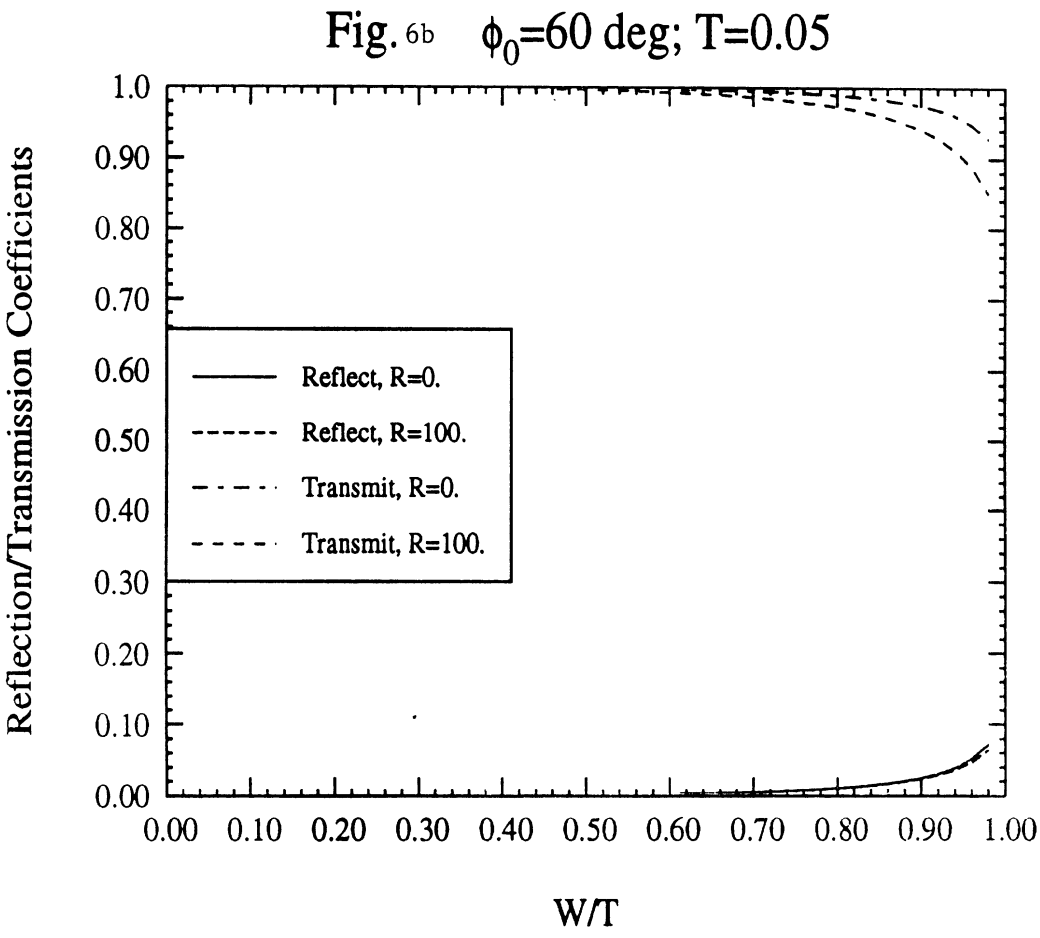

Figure 6. Plots of the reflection and transmission coefficients for an infinite resistive strip array as a function of w/T using the formulae (19) and (20): (a) $T = 0.1\lambda$; (b) $T = 0.05\lambda$.

Fig. 7a T=0.5λ

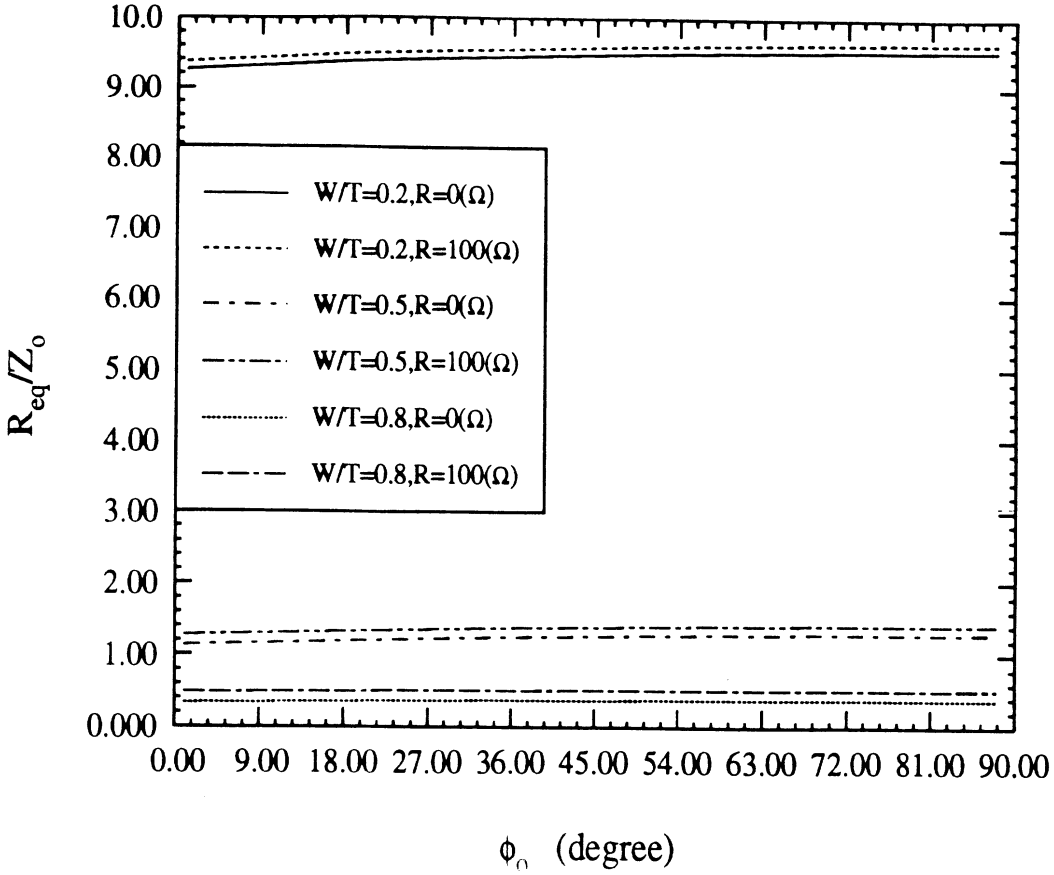

Fig. 7b T=0.2λ

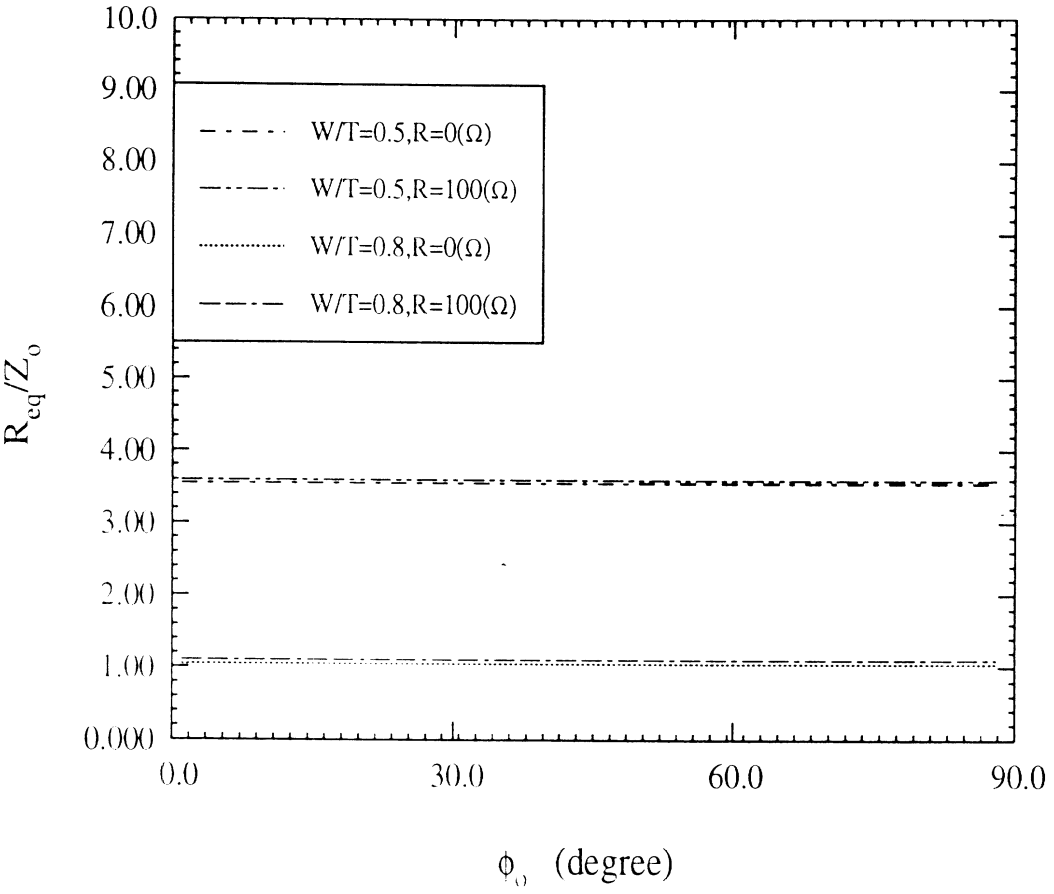

Figure 7. Plots of the equivalent sheet impedance R_{eq} as a function ϕ_0 for three different values of w/T.

Fig. 8a

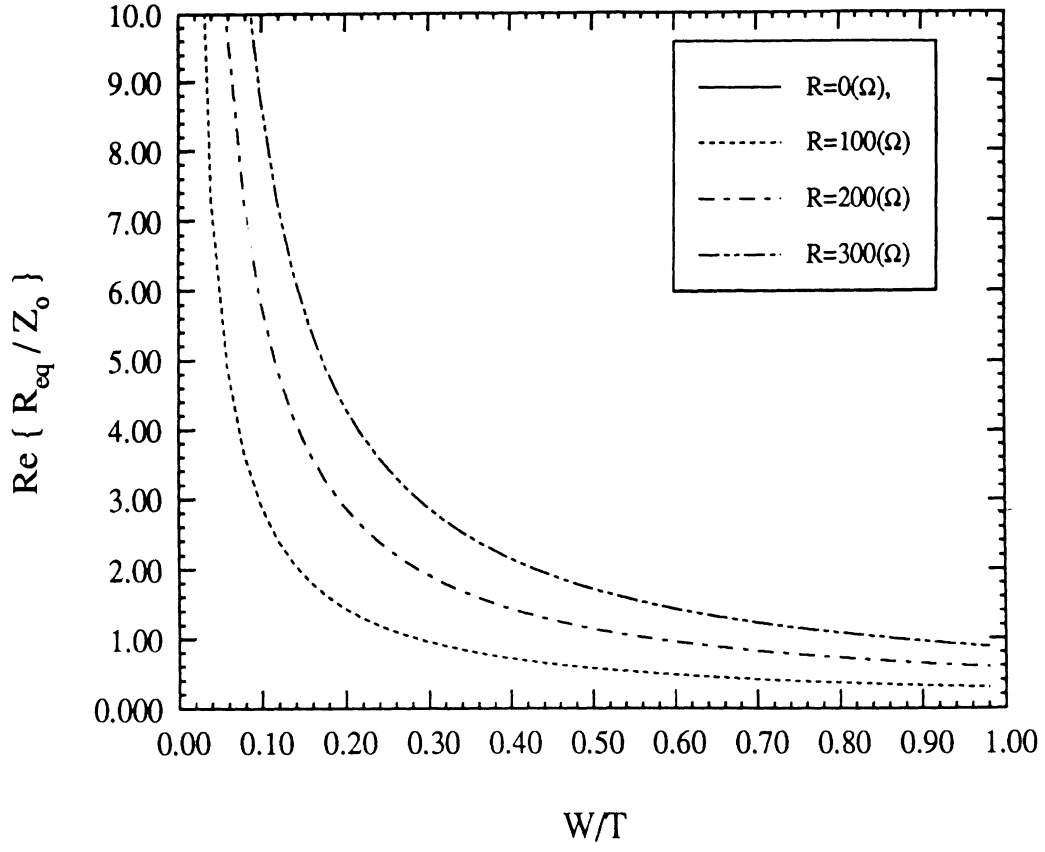

Fig. 8b

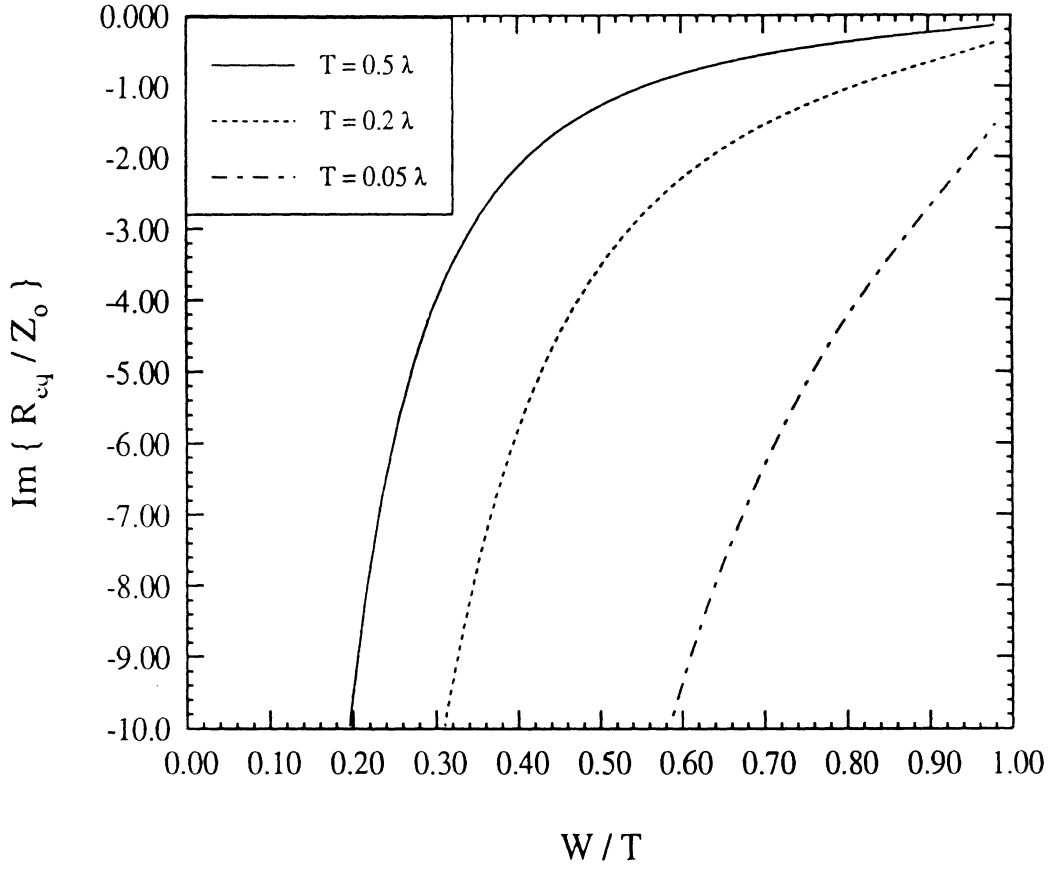

Figure 8. Plots of the equivalent sheet impedance $\tilde{R}$ of the resistive strip array as a function of w/T ($\phi_0 = 60°$): (a) real part (holds for all values of T; (b) Imag. (holds for all values of R).

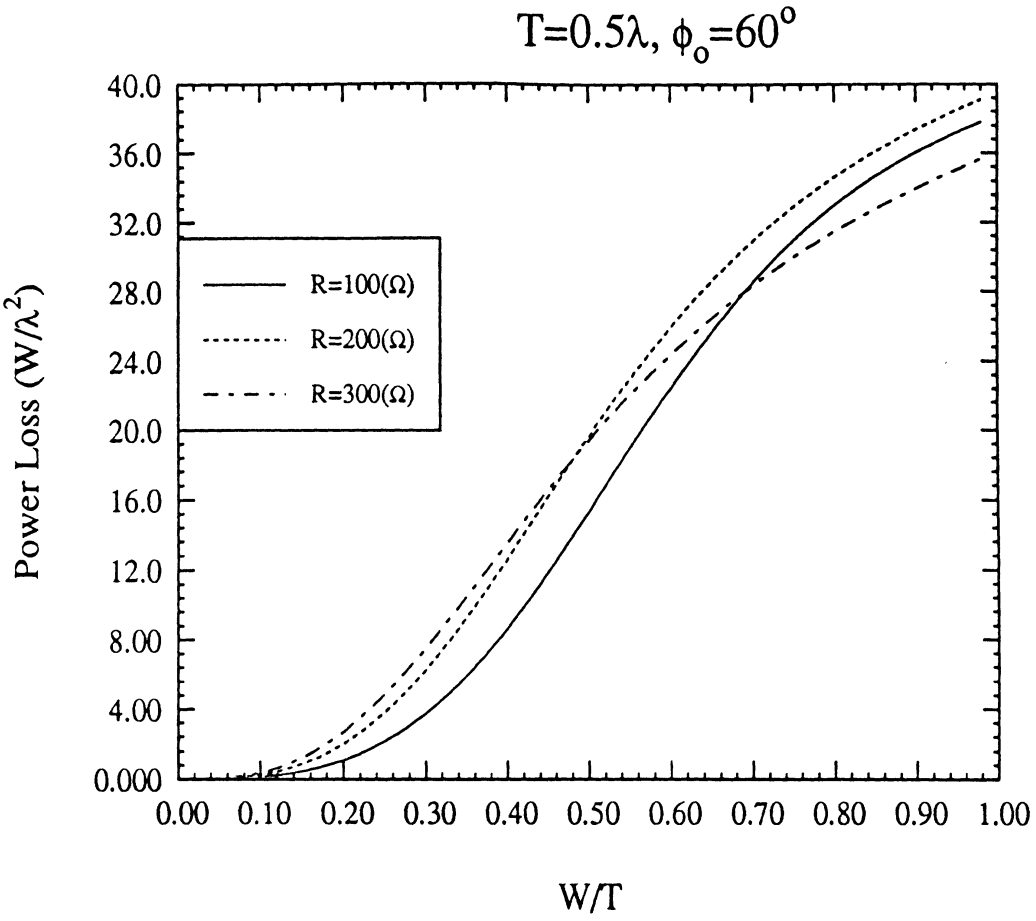

Figure 9. Plots of the absorbed power per square wavelength as a function of w/T with $T = 0.5\lambda$.

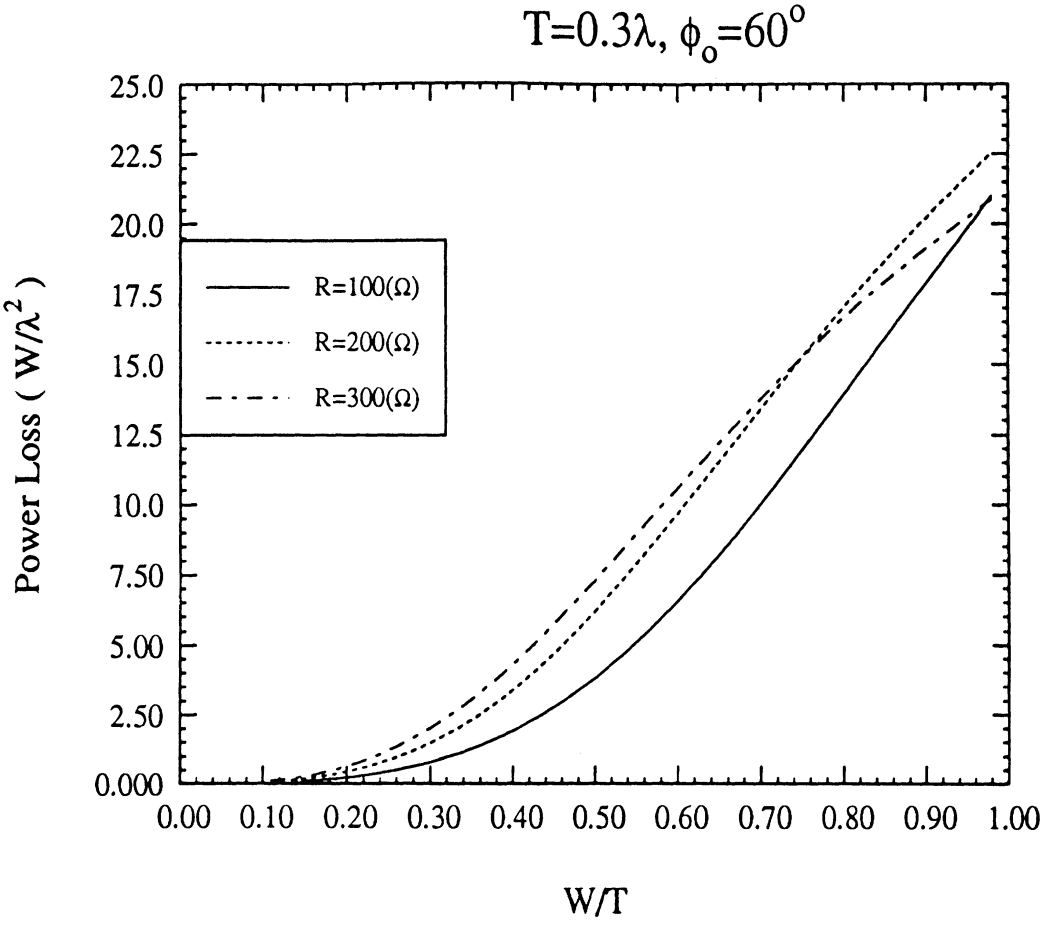

Figure 10. Plots of the absorbed power per square wavelength as a function of w/T with $T = 0.3\lambda$.

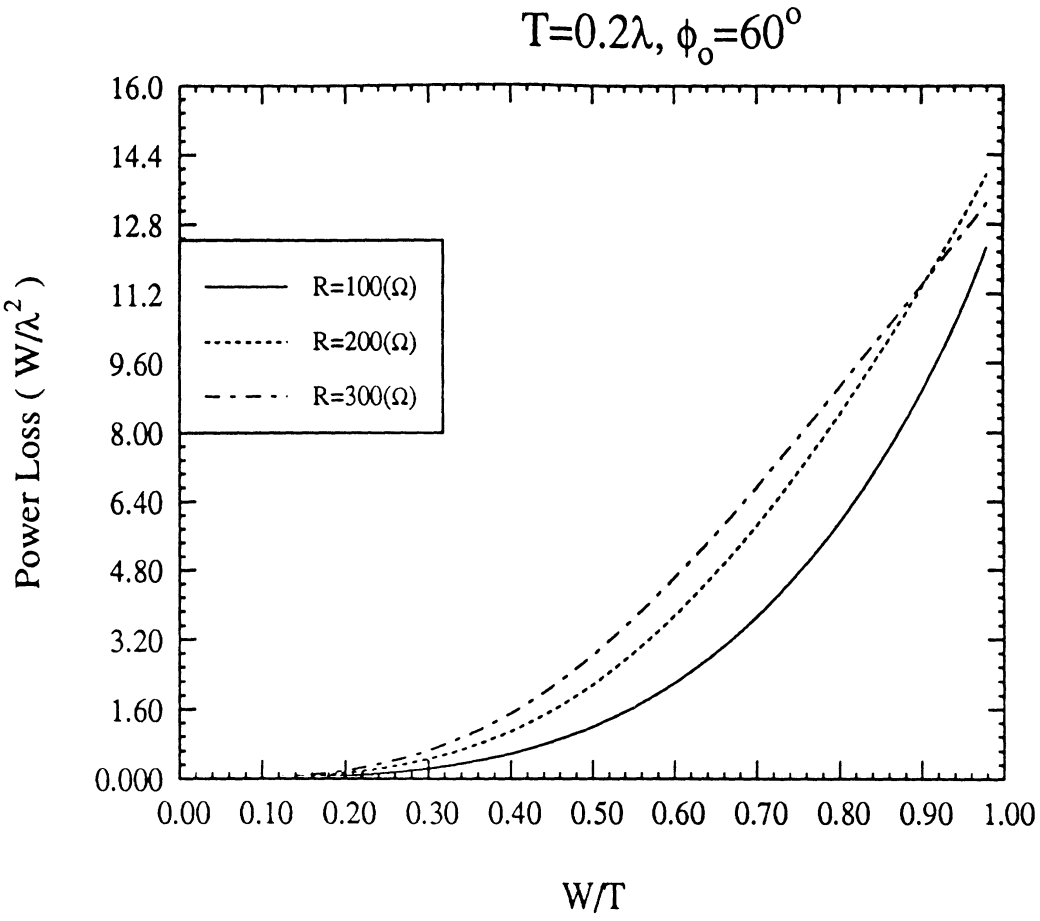

Figure 11. Plots of the absorbed power per square wavelength as a function of w/T with $T = 0.2\lambda$.

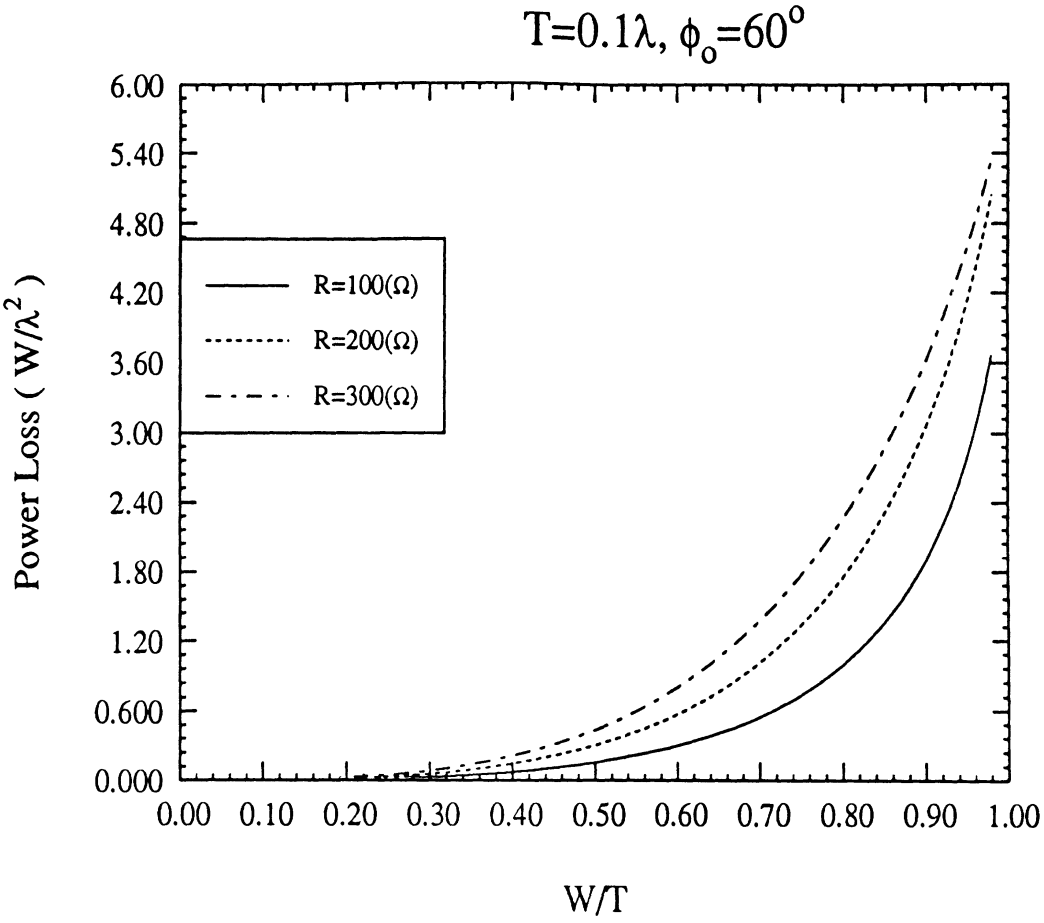

Figure 12. Plots of the absorbed power per square wavelength as a function of w/T with $T = 0.1\lambda$.

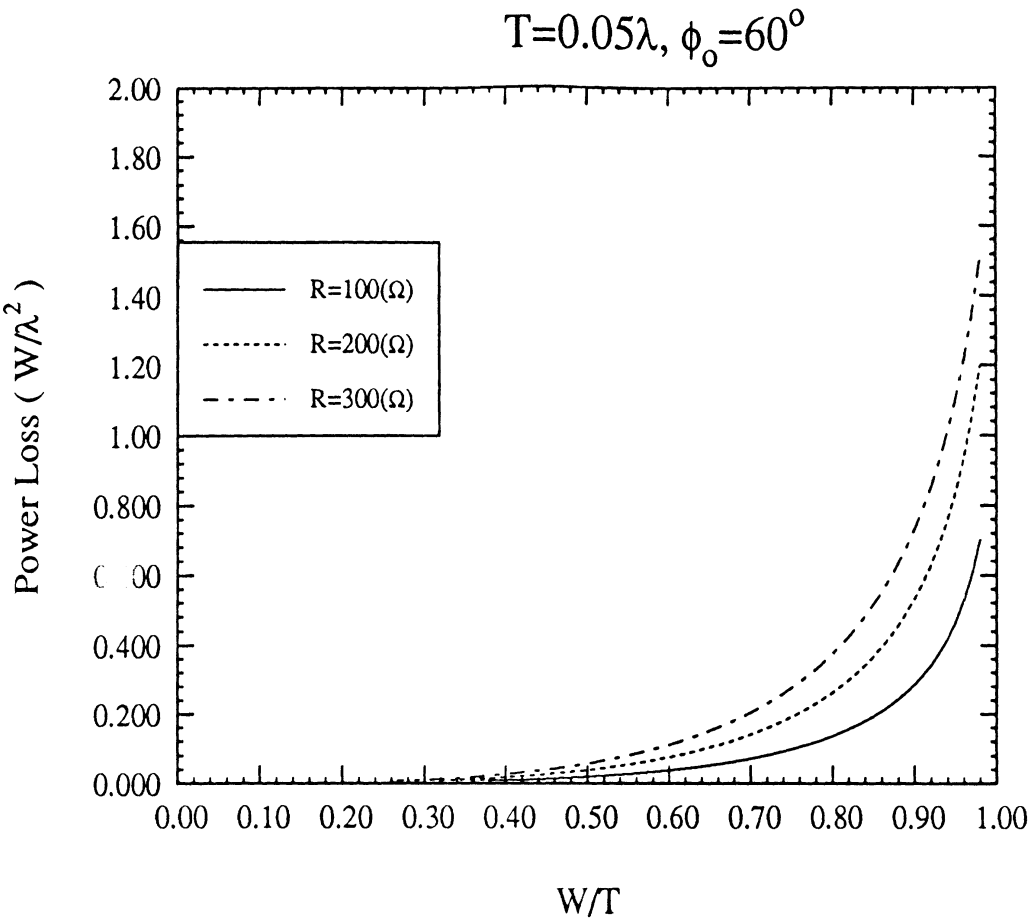

Figure 13. Plots of the absorbed power per square wavelength as a function of w/T with $T = 0.05\lambda$.

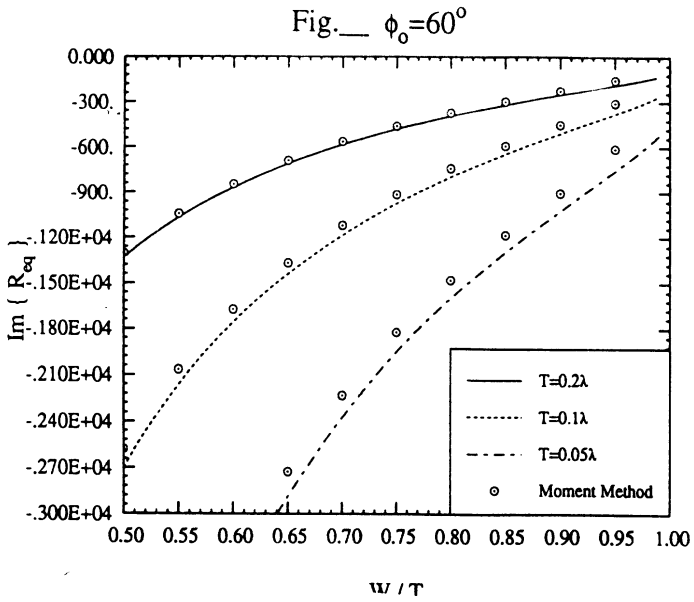

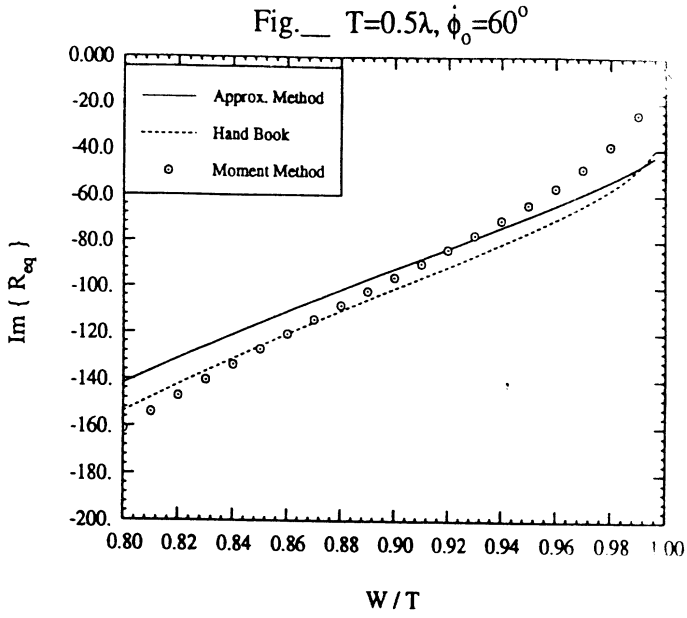

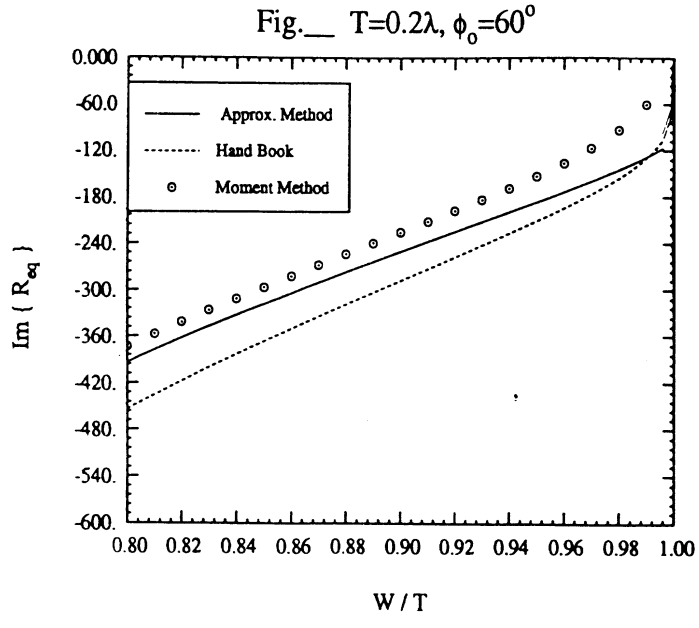

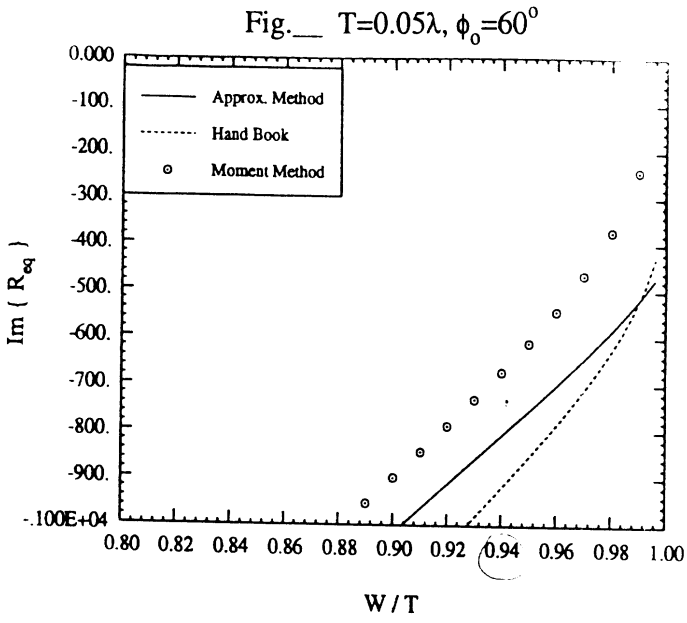

Figure 14. Reactive part of R_{eq} as a function of W/T. Note that Im$\{R_{eq}\}$ is independent of the resistivity R.

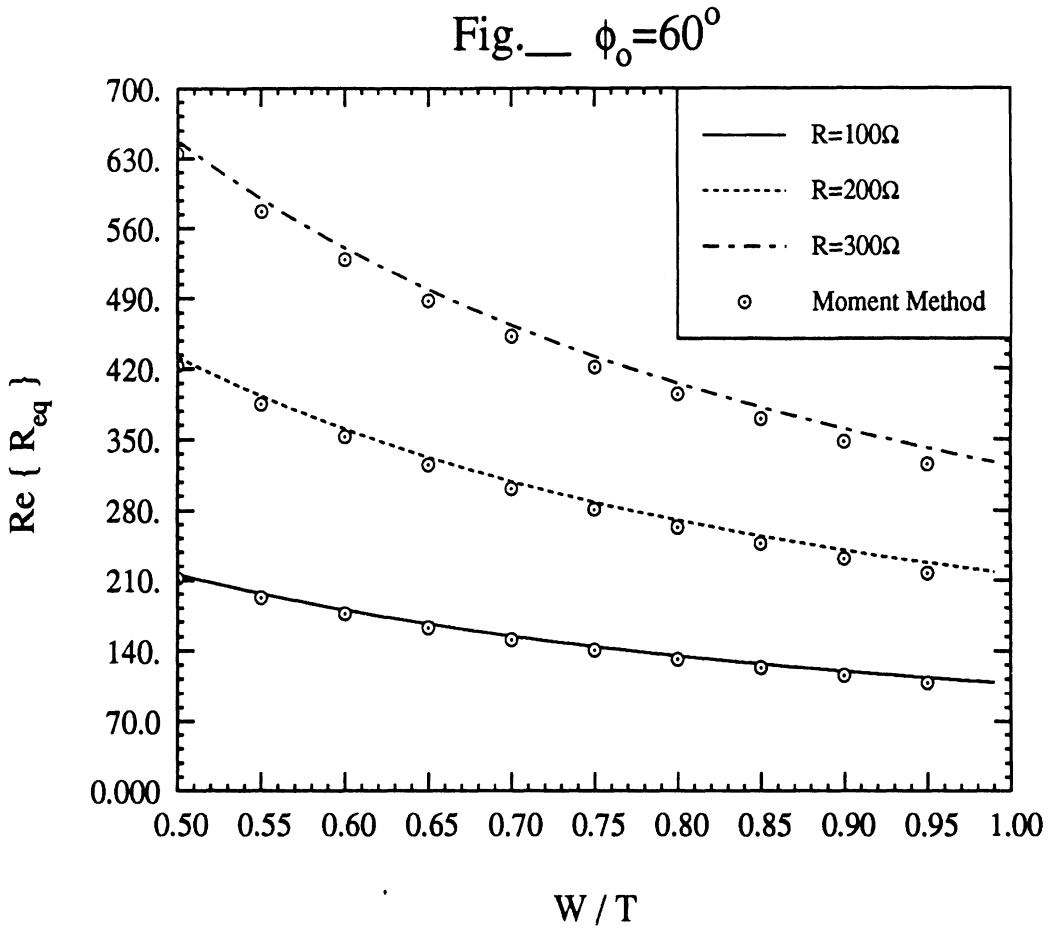

Figure 15. Real part of R_{eq} as a function of W/T for different values of R. Note that Re$\{R_{eq}\}$ is independent of the period T.